ACS APPLIED MATERIALS & INTERFACES

www.acsami.org

Research Article

Silanization of Plasma-Activated Hexamethyldisiloxane-Based Plasma Polymers for Substrate-Independent Deposition of Coatings with Controlled Surface Chemistry

Tim Egghe, Rouba Ghobeira, Parinaz Saadat Esbah Tabaei, Rino Morent, Richard Hoogenboom,* and Nathalie De Geyter*

Cite This: *ACS Appl. Mater. Interfaces* 2022, 14, 4620–4636

Read Online

ACCESS | Metrics & More | Article Recommendations | Supporting Information

ABSTRACT: Plasma polymerization has emerged as an appealing technique for surface modification because of its advantages over a variety of conventional techniques, including ease-of-use and the possibility to modify nearly any substrate. One of the main challenges of plasma polymer-based surface modification, however, is having control over the coating chemistry, as plasma deposition generates a diversity of chemical structures. Therefore, this study presents an alternative plasma-based method for the fabrication of coatings that contain selective functionalities. In a first step, hexamethyldisiloxane (HMDSO) plasma polymerization is performed in a medium-pressure dielectric barrier discharge (DBD) to deposit polydimethylsiloxane (PDMS)-like coatings. In a second step, this coating is exposed to an air plasma in a similar DBD setup to introduce silanol groups on the surface. These groups are used in a third and final step as anchoring points for grafting of (3-aminopropyl)triethoxysilane (APTES) and (3-bromopropyl)trichlorosilane (BrPTCS) to selectively introduce amino or bromo groups, respectively. X-ray photoelectron spectroscopy (XPS) and water contact angle (WCA) measurements indicated that the first two steps were successful. Moreover, the coating could be synthesized on three different surfaces, namely, glass, ultrahigh-molecular-weight polyethylene, and polytetrafluoroethylene, indicating the wide applicability of the developed procedure. Afterward, XPS also proved that the APTES and BrPTCS grafting resulted in the formation of a coating containing primary amines and alkyl bromides, respectively, in combination with an organosilicon matrix containing silanol groups as remaining reactive groups, proving the successful synthesis of selective functional plasma-based coatings. The intermediate air-plasma-activation step was demonstrated to be necessary for successful and stable grafting of the final layer. In conclusion, this study established a general procedure for the development of coatings with selective functionality that can be applied on a wide variety of substrates for, e.g., biosensor applications, biomolecule, or polymer immobilization or for the synthesis of antibacterial coatings.

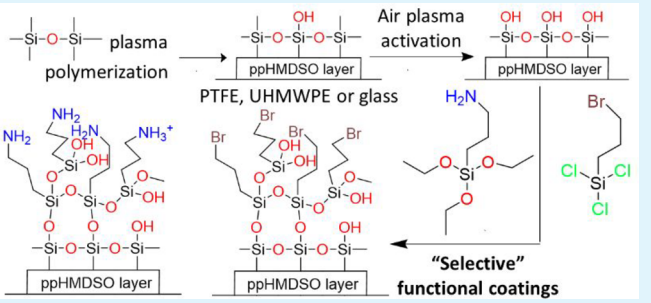

KEYWORDS: *plasma polymerization, plasma activation, hexamethyldisiloxane, silanization, (3-aminopropyl)triethoxysilane, (3-bromopropyl)trichlorosilane, selective functionality*

1. INTRODUCTION

The surface chemical properties of a variety of materials need to be optimized to obtain an optimal performance in a wide range of applications, including biomedical and energy storage devices.[1] As such, applying a coating that contains suitable chemical functionalities is among the most used modification strategies to alter the surface chemistry of a material.[2,3] An ideal coating can be applied on a wide range of materials and is stable under the applied conditions, which is not attainable for a variety of conventional techniques.[2] Among the widely applicable coating approaches, polydopamine (PDA)-based techniques and plasma-enhanced chemical vapor deposition (PECVD) have attracted much attention because they are cost-effective, environmentally friendly, and often one-step procedures.[4,5] PECVD, and in general plasma polymerization, offer an additional advantage residing in the fact that a variety of different coatings with desired characteristics can be obtained by selecting the monomer and optimizing the plasma parameters. A wide variety of functionalities can be employed, and the applications range from barrier layers to cell adhesion-altering coatings for implants and biosensors.[4,6−8]

During a plasma polymerization process, organic compounds (often called precursors or monomers) are introduced

Received: September 21, 2021
Accepted: December 21, 2021
Published: January 11, 2022

in a nonthermal plasma, which leads to their fragmentation and recombination in the plasma phase and on substrates that are placed in (the vicinity of) the ionized gas. The latter process leads to the deposition of cross-linked, submicrometer thin coatings.[4] One of the main challenges for plasma polymerization methods is to obtain good control over the coating chemistry, as the aforementioned fragmentation pathways result in poor chemical selectivity in the deposited layer. This makes the implementation of these coatings more challenging for applications in which a well-defined chemistry or high density of a specific functional group is required for optimal performance, like for biosensors and biomolecule or polymer immobilization.[9,10] In order to optimize this selective functional group density, most studies select a monomer containing the desired functionality, after which the functional group retention is maximized by optimizing the plasma parameters.[4,11] Particularly interesting is the use of pulsed treatment cycles for this purpose, although synthesizing coatings with one specific functionality remains very challenging.[12]

Friedrich et al. developed an alternative two-step method to form "monotype functional" coatings with a significantly improved chemical selectivity. This method comprises the deposition of a bromine-based plasma polymer coating, after which diamines, diols, dithiols, or sodium azide can react with the C−Br bond to form "monofunctional" alcohol, amine, thiol, and azide surfaces, respectively.[13−15] The concept is based on the specific chemistry of bromine-based plasma polymers, as a high C−Br selectivity can be obtained because of the electronic configuration of Br that only allows a single bond with carbon. This is in contrast to other precursor types like amines, in which a variety of N-containing groups, such as amines, nitriles, and amides, are introduced in the resulting coating.[16] A selectivity of up to 95% in C−Br, although not clarified if it concerns primary, secondary, or tertiary alkyl bromide groups, can be obtained which can subsequently be used to anchor specific functionalities.[13] It should however be noted that a complete reaction of alkyl bromide functionalities was not achieved and that due to the retention of bromide, not one but two functional groups were present at the surface. Therefore, these types of coatings will be referred to as possessing "selective functionality" instead of "monofunctionality". Nonetheless, this is still a major improvement of conventional plasma polymer coatings that contain a much broader variety of functional groups.[14]

This paper reports a new method for the fabrication of "selective functional" plasma polymer-based coatings. The approach is based on the substrate-independent deposition of a silanol-containing layer which can subsequently react with a silane coupling agent to introduce a particular functional group. Even though silane coupling agents are widely used for modification of inorganic substrates like silica and glass, they have not yet been combined with plasma-polymerization derived coatings that can be applied to both inorganic and organic substrates.[17−21] In this regard, it is important that different precursors have already been used to synthesize glass-like plasma polymer coatings that typically contain a significant amount of silanol groups.[22,23] Reported examples of such precursors are tetraethoxysilane (TEOS), tetramethoxysilane (TMOS), and hexamethyldisiloxane (HMDSO) of which the latter is most often used because of its high vapor pressure and nontoxicity.[23,24] Typically, HMDSO needs to be mixed with O_2 (or air) to form glass-like coatings, while the plasma polymerization of pure HMDSO (with or without carrier gas) results in polydimethylsiloxane (PDMS)-like coatings.[23] The glass-like coatings can be prone to undesirable cracking because of increasing internal stresses.[25] Therefore, a plasma-activation step on PDMS-like HMDSO plasma polymer coatings, which typically lack these internal stresses, is implemented to synthesize silanol-rich coatings.[26] These coatings will then be silanized in the final step to develop "selective functional" layers where the functional group can be controlled by selection of the corresponding silanization reagent.

As such, this paper first discusses the deposition of HMDSO-based plasma polymers on three different substrates to explicitly illustrate the wide applicability of the deposition process. This step is analyzed by water contact angle (WCA) measurements and X-ray photoelectron spectroscopy (XPS). Thereafter, air-plasma activation of these layers is investigated to increase the amount of surface silanol groups, which is analyzed by the same techniques. As a third step, the silanization reaction of the plasma-activated HMDSO-based coatings and two model silane coupling reagents, (3-aminopropyl)triethoxysilane (APTES) and (3-bromopropyl)-trichlorosilane (BrPTCS), is studied as a function of time, which is followed by XPS. For one selected reaction time, the influence of the plasma-activation step on the reaction and the coating stability is also examined.

2. MATERIALS AND METHODS

2.1. Materials. Ethanol (EtOH) (Rotisol V, HPLC grade), acetone (99.5%), and toluene (≥99.5%) were purchased from Carl Roth. APTES (99%) and BrPTCS (90%) were purchased from Merck. HMDSO (≥98%) was purchased from Acros Organics. Argon (Ar) (Alphagaz 1) and dry air (Alphagaz 1) were purchased from Air Liquide. All chemical and gases were used as supplied. Glass coverslips (diameter: 12 mm, thickness: 0.13−0.16 mm) were purchased from VWR. A roll of ultrahigh-molecular-weight polyethylene (UHMWPE) (thickness: 0.075 mm) film and a roll of polytetrafluoroethylene (PTFE) (thickness: 0.1 mm) film were obtained from Goodfellow. Samples of 2.5 cm × 2.5 cm were cut out for plasma polymerization treatment and used without any pretreatment.

2.2. Plasma Processes. *2.2.1. Plasma Polymerization of HMDSO.* The plasma polymerization experiments were performed in a medium-pressure dielectric barrier discharge (DBD) reactor which combines the monomer evaporation mechanism and the reactor geometry of two different setups that have been described in earlier work.[27,28] The scheme of the reactor can be found in the Supporting Information (Figure S1). In short, the cylindrical plasma reactor consisted of two parallel electrodes placed 7.5 mm away from each other. The lower copper electrode was covered with a ceramic alumina layer, and the upper electrode was a porous stainless steel electrode, covered with a ceramic coating. The lower electrode was connected to a 50 kHz AC power source, while the upper electrode was connected to the ground through a 50 Ω resistor. The diameter of the electrodes was 4.5 cm. The discharge mixture consisted of a main Ar flow and the HMDSO monomer, which is introduced in the plasma reactor using a glass bubbler containing the precursor, carried by a secondary Ar flow. Both Ar flows are controlled by an El-Flow gas mass flow controller (Bronkhorst). Before the mixture entered the plasma reactor through the upper electrode, it first passed through a glass wool filler to distribute the gas flow more evenly before entering the plasma discharge region. The bottom of the plasma reactor was connected to a simple pumping unit, allowing the evacuation of the plasma reactor and subsequent filling with a reproducible atmosphere.

Three different types of substrates were used in this study. PTFE or UHMWPE samples with the aforementioned size were fixed on the lower electrode, while 4 glass substrates were placed to cover a similar area of this electrode. After placement of the substrate, the reactor was

https://doi.org/10.1021/acsami.1c18223
ACS Appl. Mater. Interfaces 2022, 14, 4620−4636

pumped down to <0.3 kPa and subsequently filled with Ar to atmospheric pressure. Thereafter, the Ar flow was set at 2000 standard cubic centimeters per minute (sccm), the valve toward the bubbling system was opened, and the secondary Ar flow was set at 2 sccm. Afterward, the reactor was pumped down to 27.5 kPa, and the gas mixture was left flowing for 1 min before switching on the high voltage power source to obtain a more reproducible equilibrium between in- and out-flow of the gas. The deposition time was 1 min for all treatments. The effective loading for the HMDSO vapor is calculated by measuring the quantity of liquid consumed within 40 min. This calibration indicated that the reactive vapor mass flow was equal to 11 mg/min, which corresponds to a concentration of 7.19 ppm of HMDSO in the carrier gas.

To electrically characterize the DBD, the applied high voltage and the resultant discharge current were measured. The high voltage applied to the lower copper electrode was measured using a 1000:1 high voltage probe (Tektronix P6015A). The discharge current was obtained by measuring the voltage across a 50 Ω resistor connected in series with the reactor to the ground. Via Ohm's law, the discharge current was calculated. The obtained waveforms were recorded using a digital oscilloscope (Picoscope 3204A), and the applied power was calculated by performing a discrete integration of the multiplication of voltage and current as described in previous work.[29] The power was 1.8 W for all treatments and did not vary when different substrates were used. A representative voltage−current plot is displayed in the Supporting Information (Figure S2A).

2.2.2. Plasma Activation of HMDSO-Based Plasma Polymer Layers. The substrates that were subjected to the plasma polymerization process were subsequently plasma activated by using a medium-pressure parallel-plate DBD reactor that was already described in previous work.[30] In short, a discharge is generated between two copper electrodes (Ø = 58 mm) covered with glass plates, acting as barrier layers. The distance between the two dielectric layers was 3.5 mm. The upper electrode is connected to a 50 kHz AC high voltage source, while the lower electrode is connected to ground via a 50 Ω resistor. The sample was put at the center of the lower electrode, parallel to the gas inlet, after which the system was pumped down to less than 0.25 kPa using a rotary vane pump. The UHMWPE and PTFE substrates which were subjected to the plasma polymerization were cut afterward in two to have two samples of approximately 1.2 cm × 2.5 cm. One sample was plasma activated each time to ensure an as homogeneous treatment as possible over the total surface. For glass, three samples were used for each plasma activation. After the sample application, the system was flushed by a dry air flow of 3000 sccm at 50 kPa for 3 min after which the reactor was brought to 5 kPa with a gas flow of 1000 sccm. Then, the plasma was ignited with a fixed applied power. The treatment time varied between 0 and 120 s. The same electrical characterization as described in the previous section was employed for this setup. A power of 2.2 W was applied for all treatments. No power variations were observed when different substrates were used. A representative voltage−current plot is displayed in the Supporting Information (Figure S2B).

2.3. APTES and BrPTCS Reaction and Stability Evaluation. Three different reaction mixtures with the same concentration (2% v/v) were used within this study: APTES/toluene, APTES/ethanol, and BrPTCS/toluene. For the first two mixtures, one sample was incubated in 5 mL of the solvent at 70 °C after which the respective amount of APTES was added. Each mixture was stirred for a certain reaction time which varied in between 5 min and 6 h. For the third mixture, one sample was incubated in 1 mL of the solvent at room temperature after which the respective amount of BrPTCS was added. Each mixture was shaken at 100 rpm for the same reaction times as mentioned before. For the reactions on the PTFE and UHMWPE samples, a piece of approximately 1 cm × 1 cm was cut out of the (plasma-activated) substrate. One coverslip was used for the reactions on glass.

To evaluate the stability of the coatings, the treated substrates were subjected to 5 min of ultrasonification in ethanol and 5 min in acetone by using a Branson 1510 Ultrasonic Cleaner. All samples were stored in vacuum before analysis by XPS or AFM.

2.4. WCA Analysis. The plasma-polymerized HMDSO coatings without and with subsequent plasma activation were analyzed by WCA measurements. These measurements were performed at room temperature, using a commercial Krüss Easy Drop system (Krüss Gmbh, Germany). After the plasma polymerization, 9 water droplets of 2.0 μL of deionized water were placed on different positions of the sample surface. After the consecutive plasma activation, 3 water droplets were used for each sample. All measurements were performed in triplicate on samples obtained in different plasma experiments. WCAs were measured within 5 min after the coating deposition or plasma-activation process.

2.5. XPS. XPS surface analysis was performed on a PHI 5000 Versaprobe II spectrometer, which used a monochromatic Al Kα X-ray source ($h\nu$ = 1486.6 eV) operating at 23.5 W. A vacuum of at least 10^{-6} Pa was obtained for all measurements. Survey scans and high-resolution spectra (C 1s, N 1s, O 1s, Si 2p, Br 3d) were recorded with pass energies of 187.85 eV (eV step = 0.8 eV) and 23.50 eV (eV step = 0.1 eV), respectively, at an angle of 45° to the normal of the sample using a spot diameter of 50 μm. Four points were measured per sample. Multipak (v9.6.1) was used for elemental analysis using a Shirley background and employing the relative sensitivity factors as supplied by the manufacturer. The calibration of high-resolution XPS spectra was also performed in Multipak. The C 1s spectra were calibrated at 284.4 eV (C−Si bond) for the plasma-polymerized HMDSO coatings and their air-plasma-activated equivalent, as described before.[31] For the APTES- and BrPTCS-modified coatings, the C 1s spectra were calibrated at 285 eV, because of the increased contribution of the C−C bond. For a qualitative comparison of the high-resolution XPS spectra in between the different treatments, the binding energies were obtained from literature and displayed on the spectra. A summary can be found in Table 1.[14,31−33] SiO_x will be further used to indicate a silicon connected to X O's and $(4-X)$ C's. For the N 1s spectra, deconvolutions using Gaussian−Lorentzian peak shapes with the mentioned peak energies, a fwhm of 1.5−1.6 eV, and χ^2 below 2 can be made, indicating that this peak is mainly constituted of C−NH_2 and C−NH_3^+ bond contributions. For the Br 3d spectra, deconvolutions using Gaussian−Lorentzian peak shapes with peak energies at 70.1−70.3 eV and 71.2−71.3 eV for, respectively, Br $3d_{5/2}$ and Br $3d_{3/2}$, a fwhm of 1.0−1.3 eV and χ^2 below 2 can be made, indicating that this peak can be completely associated with C−Br bonds.

Table 1. Binding Energies Used for the Qualitative Analysis of High-Resolution XPS Spectra

C 1s		Si 2p		N 1s	
bond	binding energy (eV)	bond	binding energy (eV)	bond	binding energy (eV)
C−Si	284.4	SiO	101.5	C−NH_2	399.3
C−C	285	SiO_2	102.1	C−NH_3^+	400.9−401.0
C−N	285.7	SiO_3	102.8		
C−Br	285.9	SiO_4	103.4		
C−O	286.6				
C═O	287.7				
COOH/COOC	289.4				

2.6. AFM. The influence of the different steps in the coating fabrication on the surface morphology and roughness has been investigated by AFM. All measurements were performed by an XE-70 atomic force microscope (Park Systems), used in the noncontact mode with a silicon cantilever (Nanosensors PPP-NCHR). XEI software was used for surface roughness analysis after a leveling procedure. For glass, ppHMDSO, air-plasma-activated ppHMDSO (apa-ppHMDSO), and APTES-modified apa-ppHMDSO samples, a leveling procedure that uses a first regression line-flattening procedure in the x-direction (fast scanning axis) in which the fragments (highest

https://doi.org/10.1021/acsami.1c18223
ACS Appl. Mater. Interfaces 2022, 14, 4620−4636

Table 2. WCAs for Untreated Samples and WCAs and XPS Atomic Compositions for the ppHMDSO Coatings on Three Substrates

	WCA (deg)		XPS		
	untreated	ppHMDSO	C%	O%	Si%
UHMWPE	99.0 ± 1.8	107.5 ± 1.7	53.1 ± 0.6	23.8 ± 0.9	23.1 ± 0.3
PTFE	120.6 ± 2.9	106.4 ± 2.7	53.7 ± 0.2	24.2 ± 0.4	22.1 ± 0.6
glass	72.0 ± 2.5	106.2 ± 1.7	52.9 ± 1.0	24.2 ± 1.1	23.0 ± 0.2

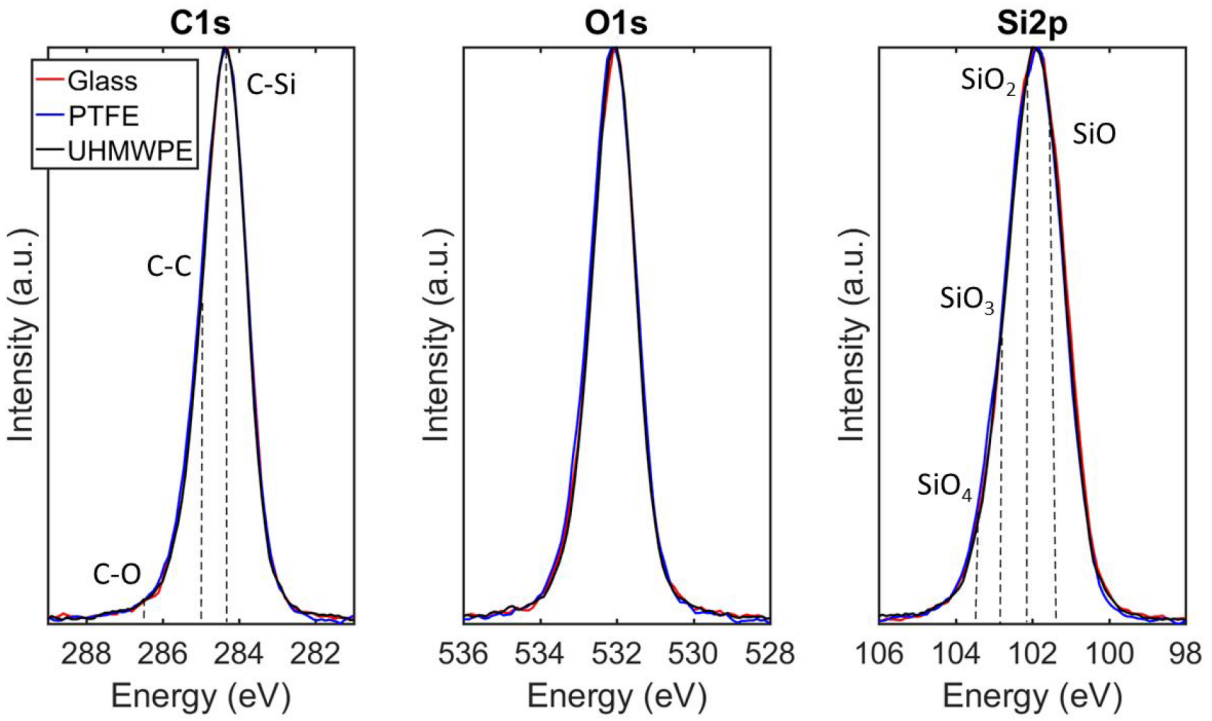

Figure 1. High-resolution XPS spectra of the ppHMDSO coating on three different substrates.

points of the sample) are excluded, was applied to the recorded images because of the relative flatness of the samples. For the BrPTCS-modified apa-ppHMDSO samples, a second-order regression plane fit in the *y*-direction (slow scanning axis) was employed to compensate for the drift without introducing artifacts that could originate from the sample inclination. For each condition, three samples with three different regions of interest on each sample were investigated. Root mean square roughness (Rq) values are presented as the average over these nine measurement points. The thickness of the plasma polymer was measured by making a scratch in the coating deposited on glass, as performed in a previous study.[4] In short, the thickness was determined by measuring the average difference in height on both sides of the scratch over 5 μm. The result is the average of three measurements on three different samples, resulting in nine total measurement points.

3. RESULTS AND DISCUSSION

3.1. Plasma Polymerization of HMDSO on Different Substrates. One main advantage of plasma polymerization is that it is applicable on a wide variety of substrates. Vasilev et al. even demonstrated that the plasma polymer composition becomes substrate-independent after deposition of a couple of nanometers, illustrating that the coating properties only depend on the process parameters and not on the substrate in their low-pressure RF plasma reactor.[34] In the medium-pressure DBD reactor that is employed in this study, it is, however, possible that the application of a material on the electrode results in an altered electrical field, which could influence the surface chemistry. Therefore, the substrate-independence of the plasma polymerized HMDSO (ppHMDSO) layers was investigated first by analyzing the coatings on three different substrates. Table 2 summarizes the WCA and XPS measurements for the ppHMDSO coatings on UHMWPE, PTFE, and glass.

It is clear that the wettability of the three substrates changed to a very similar value after the plasma-deposition of HMDSO. Also the atomic composition of the different substrates is very comparable as measured by XPS. This illustrates that the plasma polymerization process is indeed substrate-independent and the surface properties will be determined by the ppHMDSO coating. These results also indicate that the WCA values are mainly determined by the surface chemistry and not by the underlying surface morphology of the different substrates. The absence of a F-signal on the PTFE substrates also shows that the surface is completely covered. This is in line with AFM scratch measurements, which were performed as described in section 2.6. These measurements indicated that the coating thickness after 1 min of deposition on glass was equal to 94 ± 19 nm. As such, the XPS atomic composition of the ppHMDSO films is originating completely from the coating and not the underlying substrate, as the XPS analysis depth is approximately between 5 and 10 nm.[35,36] The standard deviations for WCA and XPS measurements are also lower than 3° and 1.2%, respectively, illustrating a homogeneous coating deposition over the total substrate surface.

https://doi.org/10.1021/acsami.1c18223
ACS Appl. Mater. Interfaces 2022, 14, 4620−4636

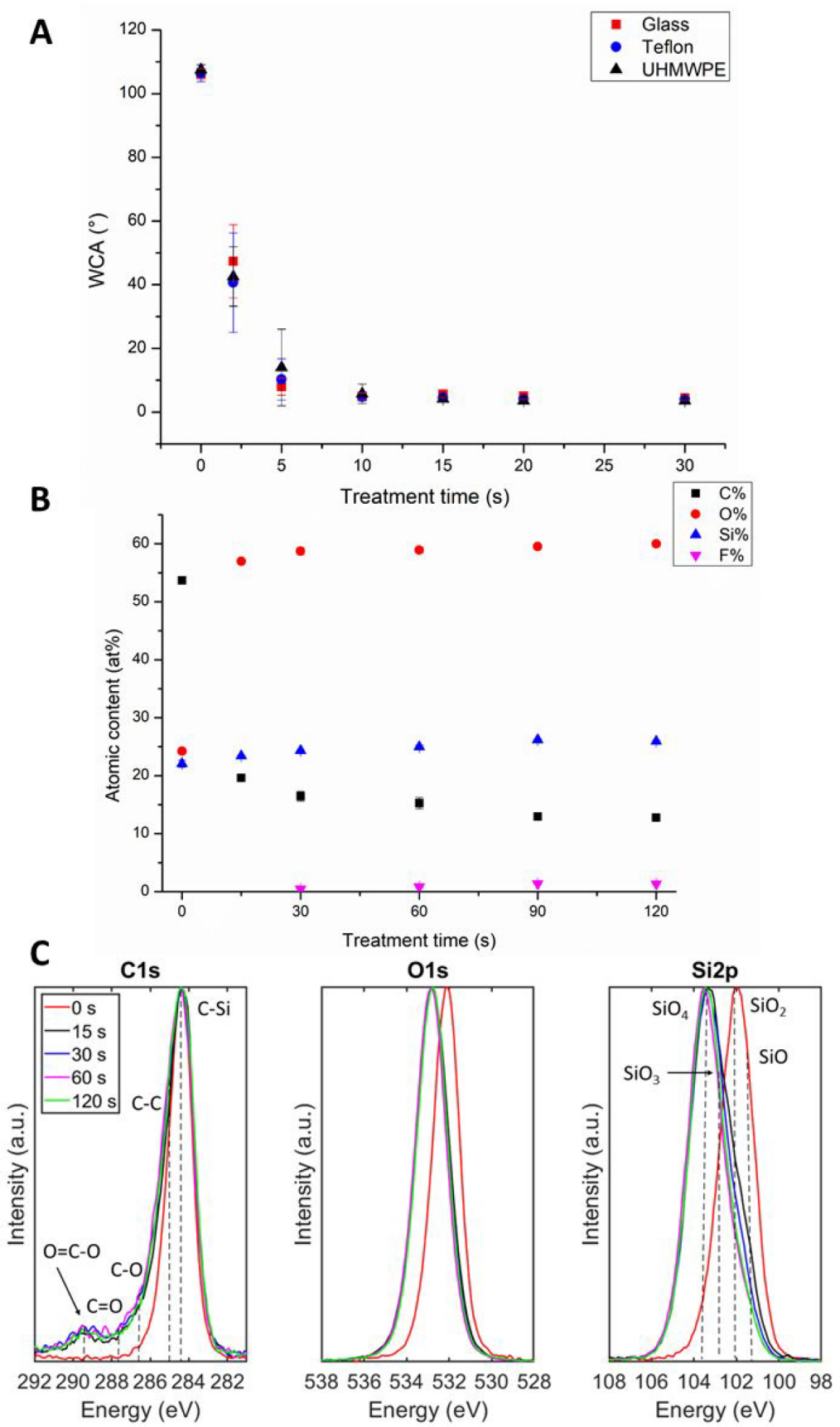

Figure 2. (A) WCAs as a function of treatment time for the air-plasma activation of ppHMDSO coatings on three substrates. (B) XPS atomic composition as a function of treatment time for the air-plasma activation of ppHMDSO coatings on PTFE. (C) High-resolution XPS spectra for different times of air-plasma activation on ppHMDSO coatings, deposited on PTFE substrates.

https://doi.org/10.1021/acsami.1c18223
ACS Appl. Mater. Interfaces 2022, 14, 4620−4636

Figure 1 displays the high-resolution XPS spectra of the relevant atoms on the three substrates.

As expected from the atomic composition, also the high-resolution XPS spectra are very similar as only a minor difference is observed in the Si 2p spectrum of PTFE coated with a ppHMDSO layer, which might be a standard variation of the process rather than an influence of the substrate. This further illustrates that applying different substrates does not influence the deposition of the ppHMDSO coatings. It is clear that the atomic composition of the coatings resembles the composition of PDMS, which has a C-, O-, and Si-content of 50%, 25%, and 25%, respectively. Also the high-resolution XPS spectra suggest that the coatings are PDMS-like, as the peak locations are in good agreement with the respective bonds of PDMS. The C 1s spectra show that C−Si bonds are most prevalent, although also C−C bonds could be present in the coating. This is however less likely as this would require a two-step degradation and cross-linking process to obtain a Si-CH_2−CH_3-like structure. Also a slight oxidation of carbon is observed around 286.6 eV, which relates to bonds like ethers and alcohols.[32] The Si 2p spectra show that SiO_2 is most prevalent in the coating, although other oxidation states will also be present according to the reference values of Alexander et al.[31] O 1s spectra are more challenging to analyze because reference studies did not focus on these as much as on the C 1s and Si 2p spectra. Therefore, these spectra are not compared to reference values, but the presented measurements are in good agreement with the observation that the coating is PDMS-like, as the peak is located at 532.1 eV. This is close to 532.4 eV, which is the reported value for Si−O−Si bonds in PDMS.[37] The broadness of the peak however also suggests the presence of C−O, which is in line with the C 1s spectra, and possibly Si−O−C and/or Si−OH bonds.[32] These results are also in line with previous work on a similar DBD setup by Morent et al.[38] They obtained a WCA of 107° after deposition on polyethylene terephthalate (PET) substrates, which is similar to this work. The reported atomic composition was, however, significantly different as the C%, O%, and Si% values were equal to 34.2%, 35.4%, and 30.4%, respectively. Nevertheless, they observed that the obtained coatings were also PDMS-like via XPS and Fourier-transform infrared (FTIR) spectroscopy. They additionally observed no silanol groups with FTIR in the PDMS-like coating. Because the atomic composition of the coatings obtained in this work is even more closely related to the composition of PDMS, it can be concluded that the presented plasma polymerization process is capable of depositing PDMS-like coatings on a variety of substrates. Importantly, no cracking was visually observed after HMDSO plasma polymerization, indicating that PDMS-like coatings are obtained rather than glass-like coatings. However, the amount of silanol groups in the coating is probably low, if these groups are even present at all. Therefore, an air-plasma-activation step of these coatings was performed to oxidize the surface before further modification, as discussed in the following section. Air was chosen within this study because of its inexpensiveness as opposed to other gases, which can introduce O-based functionalities on a surface (like He and Ar).

3.2. Air-Plasma Activation of PDMS-Like Coatings. The first step in the investigation of the air-plasma activation is the evaluation of the wettability trend as a function of treatment time, as this is a well-established method for finding the surface chemistry equilibrium state. Indeed, the surface chemistry, and as a result the wettability, does not change significantly anymore after a certain plasma treatment time, making additional treatment unnecessary.[30,39] This equilibrium state can be ascribed to the occurrence of plasma etching as the surface chemistry will no longer change during etching, as long as the underlying substrate is not exposed. Figure 2A shows the course of the WCAs as a function of treatment time for the ppHMDSO coatings on the different substrates.

As can be observed in Figure 2A, the wettability significantly increases upon plasma treatment. At 2 and 5 s, the WCAs are not uniform, which leads to standard deviation values up to 15.6°. After 10 s of treatment, the WCAs saturate around a value of 5°, which is close to the device detection limit and relates to an almost complete wetting of the surface. This already suggests the formation of polar groups like silanols on the surface. Additionally, the WCAs are homogeneous over the total sample surface which relates to a homogeneous chemistry over the total surface. The wettability trend is also very similar for the different substrates, suggesting that a similar chemistry is introduced regardless of the used sample. Therefore, all further measurements will be conducted on PTFE, because fluorine (F) would become measurable with XPS if (part of) the coating is lost. As such, the XPS measurements can serve as stability evaluation by using F as a marker. The WCA measurements depicted in Figure 2A also suggest that the plasma activation is a substrate-independent process. Figure 2B displays the trend in atomic composition of the ppHMDSO coating on PTFE as measured by XPS as a function of treatment time. The treatment times under study are extended because the WCA measurements could not indicate if the surface chemistry reached its equilibrium. It can be observed that the C-content significantly decreases while the O-content significantly increases in the first 15 s. Afterward, both contents still rise to, respectively, 12.9 ± 0.3% and 59.5 ± 0.2% at 90 s, which is very comparable to the values obtained at 120 s. The Si-content slightly increases from 22.1 ± 0.6% for the untreated ppHMDSO to 26.2 ± 0.2% after 90 s of treatment. From 30 s of treatment time onward, a small amount of F can also be found on the surface, which is most likely caused by etching of PTFE and redeposition of F-containing particles. This is however undesirable, as the presence of F should be a marker in the next sections for the stability of the coating. Therefore, an air-plasma treatment of 15 s was selected to activate the ppHMDSO coatings for subsequent silanization, as the most significant plasma activation occurred within this time frame. It should be noted that no N atoms were introduced on the surface for all plasma-activation times. This indicates that reactive O species are mainly responsible for the observed change in surface atomic composition. Similar changes in XPS atomic composition, namely a significant decrease and related increase of C- and O-content, respectively, were observed before for oxygen plasma treated PDMS.[40]

Figure 2C shows the high-resolution XPS spectra for the HMDSO-based plasma polymer and its plasma activation for 15, 30, 60, and 120 s. It is clear that the air-plasma activation modifies the ppHMDSO coating significantly. The C 1s spectra clearly show the formation of oxidized products like C−O, C═O and O═C−O, although the peak location (289.4 eV) of the latter bond is slightly higher than previously reported.[32] This formation of oxygenated carbons is typically observed after air-plasma activation, either because of reaction between the plasma active species and the substrate or because of postplasma oxidation of surface radicals after exposure to ambient air.[30,35,39] The Si 2p spectra illustrate the formation of

https://doi.org/10.1021/acsami.1c18223
ACS Appl. Mater. Interfaces 2022, 14, 4620−4636

more oxidized Si atoms as the peak shifted to higher energies. This is probably related to the dissociation of Si−C and the formation of Si−O bonds. The presence of the latter bonds suggests the presence of functional groups like Si−OH and Si−O−C. As mentioned before, O 1s spectra are more challenging to analyze, but a clear shift toward a peak value of 532.8 eV can be observed, which illustrates the different chemical environment of O atoms in the air-plasma-activated ppHMDSO (apa-ppHMDSO) layers as compared to their nonactivated equivalent. This is in accordance with the formation of C−O and O═C−O groups observed in the C 1s spectra, which typically result in a contribution around 532.8 and 533.6 eV, respectively.[32] Additionally, this shift can be related to the formation of Si−OH and Si−O−C groups that can be expected at higher energies than the Si−O−Si bond, which is located around 532.4−532.6 eV.[37] It can be observed that increasing treatment time does not have a significant influence on the C 1s and O 1s spectra, but the Si 2p spectra still show a further oxidation of Si atoms until 60 s of air-plasma activation. The measurements for a treatment time of 90 s are not shown for clarity reasons but clearly overlap with the spectra obtained at a treatment time of 60 and 120 s (see Figure S3), suggesting that no further oxidation of the Si atoms takes place after 60 s of air-plasma activation. This suggests that after 15 s of treatment, the ppHMDSO coatings did not reach its plasma activation equilibrium yet, but the most significant desired oxidation took place already. As such, these samples can be used for the subsequent silanization reactions. It should be noted that the formation of bonds such as C═O and O═C−O is believed to not interfere with the purpose of this study, as the selective functionality will completely originate from the subsequent silanization. The desired formation of silanol groups should facilitate this silanization reactions. It can also be noted that the wettability and chemistry of the plasma-activated HMDSO-based plasma polymer layers significantly differ from coatings that were plasma polymerized in an $HMDSO/O_2$ mixture, as the latter coatings showed a lower wettability and C-content compared with the apa-ppHMDSO coatings. Morent et al. obtained a constant WCA of around 28° for an increasing O_2 content in the plasma polymerization mixture in a similar DBD setup.[23] In a similar study, the same research group obtained WCA values of around 24°, and the according XPS measurements indicated a C-content of only 4%, which is significantly lower than the values in this study (19.6%−12.8%). A similar low C-content was also obtained in other setups, evidencing a different behavior between the established $HMDSO/O_2$ mixing and the oxidation of ppHMDSO coatings presented in this study.[41]

3.3. Silanization Reaction as a Function of Time. Silanization of substrates like glass and silica has been reported with a large variety of silanization agents under a wide range of reaction conditions.[42−44] In general, alkoxysilanes or chlorosilanes are the two types of agents that can be distinguished. Within this study, APTES and BrPTCS are used as model compounds for both respective types. Silanization is most often performed in nonpolar solvents like toluene, although alcohols can also be employed for alkoxysilanes.[17,18] Therefore, toluene, as the standard solvent, and ethanol, as a greener and nontoxic alternative, are selected as solvents for the reaction between APTES and the apa-ppHMDSO coatings. The reaction temperature was set at 70 °C as previous studies reported that the derived layers are more stable than those synthesized at room temperature when using a 2% v/v APTES/toluene solution.[19] In contrast, the reaction of the more reactive chlorosilanes usually takes place at room temperature.[20,21] Therefore, the reaction of BrPTCS with apa-ppHMDSO coatings was performed at room temperature, with the same concentration as the aforementioned solutions. The reaction time varies largely for both APTES and BrCPTS in between studies and therefore, the influence of this parameter on the composition of the resulting layers is first examined by XPS.[18,21,45,46] This technique can provide necessary information on the functional groups at the coatings' surface for the intended purpose, while also evaluating the stability by using the F-content as a marker. The trend in the atomic composition as a function of reaction time for the three different reaction conditions can be found in Figure 3.

Figure 3A displays the atomic composition change of the plasma-activated ppHMDSO coatings upon APTES reaction in toluene at 70 °C for different reaction times. It is clear that the C-, O-, and Si-content change significantly after a 5 min reaction time. At this time, a N-content of 11.4 ± 0.4% can be found on the surface. This indicates that the desired functionalization of the surface already took place after 5 min. However, the C- and O- contents still vary significantly until 1 h of reaction time, suggesting that reaction is still taking place, although the Si- and N-content already reached saturation after 15 min of reaction time. As such, it is evidenced that the atomic composition as measured by XPS does not change after 1 h of APTES reaction on the apa-ppHMDSO coatings in toluene at 70 °C. Figure 3B displays a similar trend for the reaction in ethanol at 70 °C, as the atomic composition varies significantly at short reaction times, before reaching a saturation at a reaction time of 3 h. It can also be observed that at short reaction times, the C- and O-content are less homogeneous than at reaction times in the saturation region, while the Si- and N-content have a similar homogeneity for all reaction times. The reaction of BrPTCS reaches a saturation almost directly, as observed in Figure 3C. The O-, Si-, and Br-content reach a homogeneous level after 30 min of reaction, while the C-content is less homogeneous as compared with the APTES reactions for most reaction times. This should however not be a problem for the intended purpose, as the Br-content is most important for a high functional group density at the surface. The absence of Cl in the XPS spectra indicates a complete reaction of the Si−Cl bonds. The higher reaction rates of these bonds in chlorosilanes over Si−O−C bonds in alkoxysilanes could explain the faster saturation of atomic composition with BrPTCS.

The absence of a significant F-signal suggests that the coatings are stable for at least 6 h in ethanol at 70 °C and in toluene at room temperature and 70 °C. The saturation for all conditions indicates that the surface reactions are either complete or that further reaction leads to an addition of a layer with similar chemistry. This will be further discussed in section 3.4. The average N-content over all measurement points was 8.3 ± 1.7% and 10.7 ± 0.8% for the APTES reactions in toluene and ethanol, respectively. This is higher than the reported values for APTES silanization on glass or silicon substrates, which ranged from 2 to 6.3%.[45,47−49] Also for BrPTCS silanization, the in literature reported value of 4.5% is lower than the observed average value in the saturation region (7.2 ± 1.0%) within this study.[50] This could be attributed to a thicker APTES/BrPTCS layer formed on the plasma polymer in comparison with other studies, which could be caused by

https://doi.org/10.1021/acsami.1c18223
ACS Appl. Mater. Interfaces 2022, 14, 4620−4636

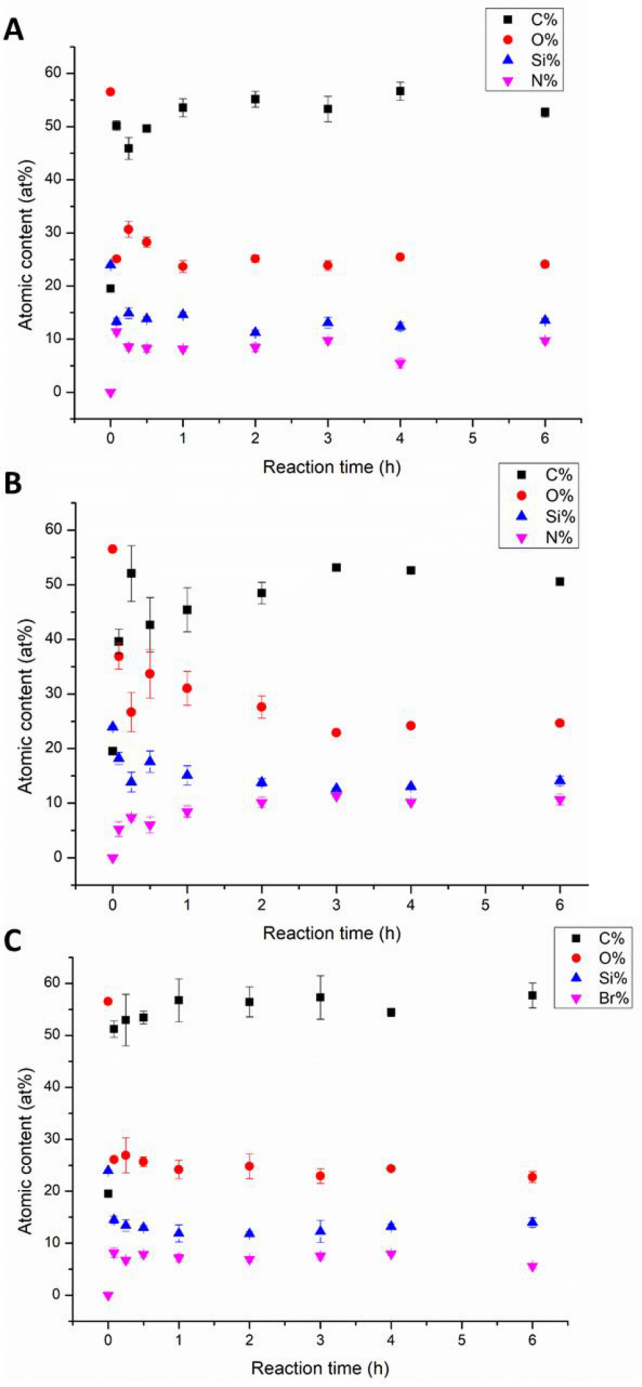

Figure 3. XPS atomic composition for the different reactions on apa-ppHMDSO coatings: (A) APTES in toluene at 70 °C, (B) APTES in ethanol at 70 °C, (C) BrPTCS in toluene at room temperature.

water traces in the reaction mixture. Indeed, the hydrolysis of Si−O−C-bonds and subsequent condensation of silanols can result in reactions between different APTES/BrPTCS molecules, followed by incorporation of these polymerized molecules in the resulting coating.[18] The relatively high N-/Br-content, together with the relatively low standard deviations for each measurement, indicate that the ppHMDSO coating is completely covered by the silanized layer. It should be noted that the formation of a thicker layer compared with more common self-assembled monolayers (SAMs) is not a problem for the selective functionality of the layer. In order to evaluate this selective functionality of the coatings, a number of representative high-resolution XPS spectra for the three different reactions are displayed in Figure 4.

Figure 4A shows the relevant high-resolution XPS spectra for a reaction time of 1, 3, and 6 h for the APTES reaction in toluene at 70 °C in comparison to the apa-ppHMDSO layers. This is, as such, a representative image of high-resolution XPS spectra in the saturation region of the atomic composition, as presented in Figure 3. The four recorded spectra for each condition are very similar, and therefore, only one spectrum per reaction time is shown. It can be observed that the spectra are very similar for the different reaction times, indicating a complete surface chemistry saturation after 1 h of reaction time. It is also clear that the high-resolution XPS spectra change significantly after the reaction. The N 1s spectra with a peak at 399.3 eV illustrate that N atoms are all incorporated as amines on the surface.[33,51] Deprotonated amines are most prevalent but a small contribution of protonated amines around 400.9 eV is also observed, which is in accordance to previously reported values.[16] The C 1s peak form is in good accordance with the expected chemistry of the aminoalkyl chain in which an equal prevalence of C−Si, C−C, and C−N is expected, although an influence of the underlying apa-ppHMDSO layer cannot be excluded.[31−33] A very small contribution of a peak around 287.7 eV was also observed, which could be associated with a very low presence of amide bonds that could originate from an oxidation of the amine.[48] The absence of C−O cannot be really proven, but if these bonds are present, the prevalence is certainly low. This indicates that most, if not all, alkoxysilanes are either hydrolyzed or reacted to form silanol or siloxane bonds, respectively. Combining N 1s and C 1s spectra proves that the APTES reaction on the apa-ppHMDSO coatings in toluene at 70 °C is capable of introducing the selective presence of amines on the surface. The Si 2p spectra are located close to the reported value of SiO_3, which is the expected oxidation state of Si for a surface composed of APTES molecules.[31] The O 1s peak shifts from 532.8 to 532.4 eV after the reaction with APTES and a considerable contribution at higher energies disappears in comparison to the O 1s spectrum of the apa-ppHMDSO coating. This probably indicates a lower presence of C−O and O═C−O, as the latter bond also disappeared in the C 1s spectra.[32] A significant contribution of Si−O−Si can also still be expected, which can be related to a poly(siloxane)-like structure by combining this observation with the observations in the Si 2p spectra. Additionally, the broadness of the peak most likely relates to the presence of Si−OH that did not undergo a condensation reaction, and/or Si−O−C groups that did not hydrolyze, but quantification is very challenging because of the aforementioned limited literature on the topic.

Figure 4B shows the relevant high-resolution XPS spectra for the APTES reaction in ethanol at 70 °C, in comparison to the apa-ppHMDSO layers. It is composed of the three reaction times in the saturation region for the atomic composition, namely, 3, 4, and 6 h. The four recorded spectra for each condition are again very similar, and therefore, only one spectrum per reaction time is shown. It is also clear that the spectra are very similar for the different reaction times, indicating a complete surface chemistry saturation after 3 h of reaction time. As such, the selective presence of amines is also proven for the APTES reaction on the apa-ppHMDSO coatings in ethanol at 70°. The same peak alterations as for

https://doi.org/10.1021/acsami.1c18223
ACS Appl. Mater. Interfaces 2022, 14, 4620−4636

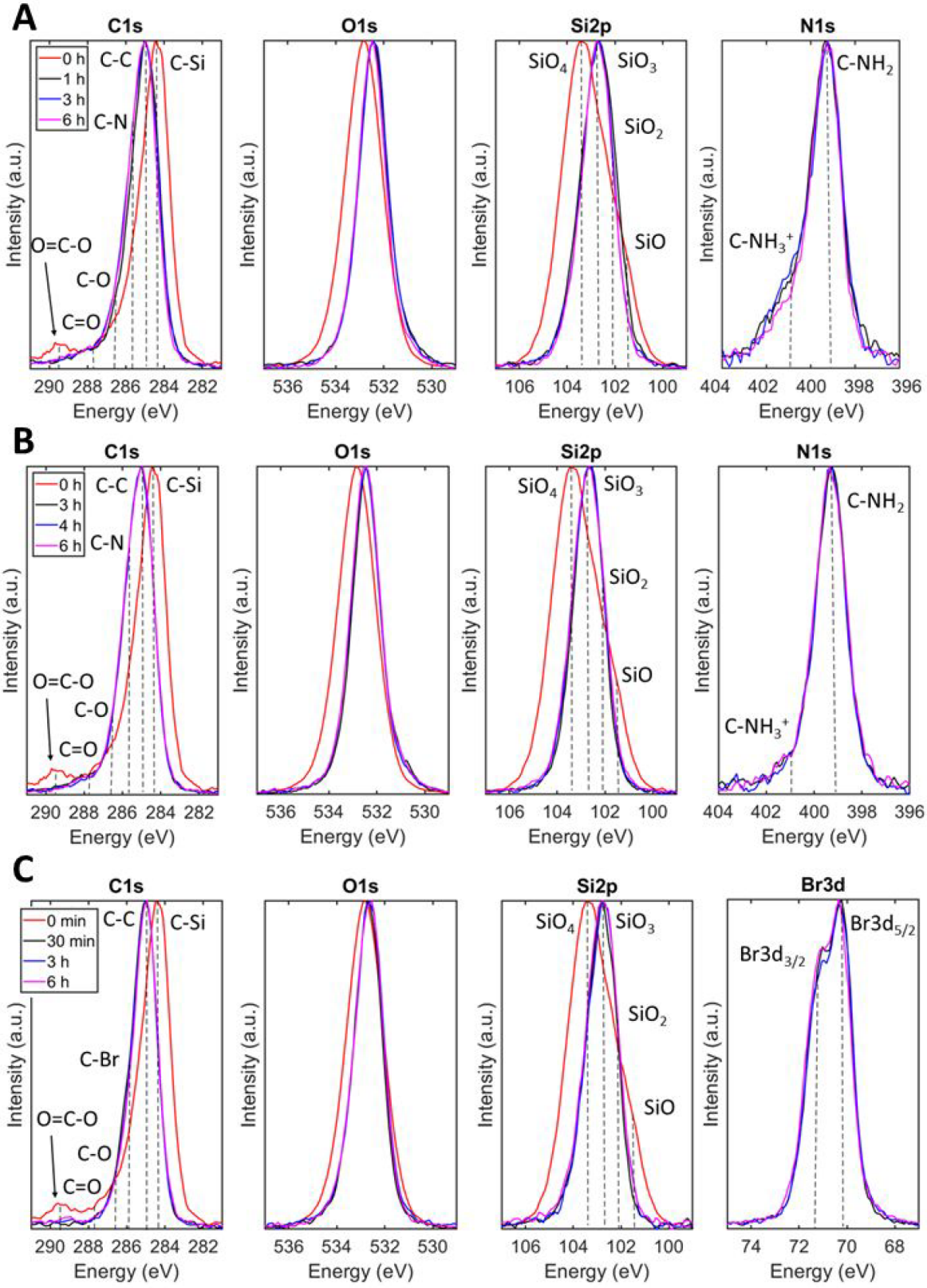

Figure 4. High-resolution XPS spectra for the different reactions on apa-ppHMDSO coatings: (A) APTES in toluene at 70 °C, (B) APTES in ethanol at 70 °C, (C) BrPTCS in toluene at room temperature.

the ATPES reaction in toluene can be observed, indicating a very similar chemistry. This is also confirmed by overlapping the APTES-modified plasma-activated ppHMDSO layers at a 3 h reaction time for both solvents. This figure can be found in the Supporting Information (Figure S4) and illustrates that mainly the amount of protonated amines differs in between the samples, which can also be observed by comparing Figure 4A,B.

https://doi.org/10.1021/acsami.1c18223
ACS Appl. Mater. Interfaces 2022, 14, 4620−4636

Table 3. XPS Atomic Composition for the Different Reactions on ppHMDSO and apa-ppHMDSO Coatings

	ppHMDSO				Apa-ppHMDSO			
	C%	O%	Si%	N%	C%	O%	Si%	N%
plasma polymer	53.7 ± 0.2	24.2 ± 0.4	22.1 ± 0.6		19.5 ± 0.2	56.5 ± 0.1	24.0 ± 0.2	
APTES 3h Tol	51.5 ± 1.0	25.4 ± 0.3	20.9 ± 0.8	2.2 ± 0.3	53.3 ± 2.4	23.9 ± 0.9	13.1 ± 1.0	9.7 ± 0.6
APTES 3h EtOh	52.2 ± 0.2	24.9 ± 0.4	21.7 ± 1.0	1.2 ± 0.9	53.1 ± 0.5	22.9 ± 0.4	12.6 ± 0.2	11.3 ± 0.2
	C%	O%	Si%	Br%	C%	O%	Si%	Br%
BrPTCS 30 min	49.2 ± 0.4	27.9 ± 0.5	15.9 ± 1.5	7.0 ± 1.3	53.4 ± 1.2	25.7 ± 0.9	13.0 ± 0.4	7.9 ± 0.6

Figure 4C shows the relevant high-resolution XPS spectra for reaction times in the saturation region of the atomic composition for the BrPTCS reaction in toluene at room temperature, in comparison to the apa-ppHMDSO layers. Similar to the above-mentioned reactions, only 1 spectrum for each reaction time, in this case 30 min, 3 and 6 h, is shown as these are representative for the other 3 spectra. The spectra are again very similar for the different reaction times, indicating a complete surface chemistry saturation after 30 min of reaction time. The Br 3d spectra with the Br $3d_{5/2}$ and Br $3d_{3/2}$ contributions around respectively 70.2 and 71.3 eV, are in good agreement with literature values for bromine covalently bonded to sp^2 and sp^3 carbon atoms, as reported for bromination of carbon black, and with the reported energy shifts for the spin−orbit splitting.[14,52] This proves the selective presence of the desired alkyl bromide chains on the surface. The C 1s peak form is in good accordance with the anticipated chemistry of the alkyl bromide chain in which an equal prevalence of C−Si, C−C, and C−Br is expected.[14,31] Similar to the previously discussed C 1s spectra, a very small contribution of a peak around 287.7 eV was observed, although the contribution is lower. The Si 2p spectra have a peak at 102.8 eV, which is in line with the expected oxidation state of trichlorosilanes that have reacted to form silanol- or siloxane-bonds (SiO_3).[31] The O 1s spectra shifts from 532.8 to 532.7 eV after the reaction with BrPTCS, and a considerable contribution at higher energies disappears in comparison to the O 1s spectrum of the apa-ppHMDSO coating. This could be again associated with a lower presence of C−O and O═C−O, as the latter bond also disappeared in the C 1s spectra.[32] The peak position is found at higher energies as compared with the O 1s peak for the APTES reactions, which could indicate a lower prevalence of Si−O−Si bonds for the BrPTCS coatings as these bonds are found around 532.4−532.6 eV.[37] It could also be related to the absence of Si−O−C groups for these coatings, but this is less likely as the presence of these bonds is rather low as observed in the C 1s spectra. The lower prevalence of Si−O−Si could be related to silanol groups that did not undergo condensation and are still present in the coating.

All the presented high-resolution XPS spectra illustrate that the coatings have a very similar surface chemistry from a certain reaction time onward. It should be noted that the XPS high-resolution spectra are less homogeneous before this saturation point, which can be attributed to the variations in the atomic composition as seen in Figure 3. This section clearly proved that the three silanization reactions were capable of introducing selective functionalities on the coating, as the only other reactive functionality except the amine- or alkyl bromide-group, could be remaining silanol groups on the surface. The next sections will use one reaction time within the saturation region to investigate the coating stability and the influence of the plasma activation on the silanization reaction. For the APTES silanization, a reaction time of 3 h is chosen for ethanol and toluene to directly compare the influence of the solvent. For the BrPTCS silanization, a reaction time of 30 min is chosen. The silanization reactions with these respective reaction times were also performed on the other substrates to illustrate that similar coatings can be obtained on a variety of surfaces (see Supporting Information, Table S1).

3.4. Influence of Plasma Activation and Coating Stability. First, the influence of the air-plasma activation on the silanization reactions is investigated, as it is possible that the ppHMDSO coatings' chemistry already allows functionalization, making the additional step unnecessary, as such. Table 3 summarizes the APTES and BrPTCS reactions on both ppHMDSO and apa-ppHMDSO coatings for the respective aforementioned reaction times.

Table 3 clearly illustrates that the APTES reaction in both solvents results in a significantly lower N-content on the ppHMDSO coatings in comparison to their air-plasma-activated equivalent. For the APTES-modified ppHMDSO coatings, the C-, O-, and Si-content do not change significantly after the reaction, while they do for the APTES-modified apa-ppHMDSO coating. These observations indicate that the reactivity between APTES and the ppHMDSO coating is much lower than between APTES and the apa-ppHMDSO coating. This results in two completely different APTES-based coatings. For the apa-ppHMDSO films, an APTES-based layer is deposited with a thickness that is slightly smaller or similar to the XPS analysis depth (approximately 5 to 10 nm).[35,36] Indeed, the fact that Si% > N% indicates a contribution of the underlying coating with higher Si-content than the APTES-based top layer. As such, the surface chemistry as measured by XPS is mainly determined by the polymerization of APTES molecules on the apa-ppHMDSO coating. For the ppHMDSO films, a significantly lower amount of APTES molecules are immobilized on the plasma polymer, as evidenced by the low N-content. The C-, O-, and Si- content does not change significantly, indicating that a thin layer of APTES molecules is deposited and that the surface chemistry is mainly determined by the underlying ppHMDSO coating.

On the other hand, the BrPTCS reaction results in very comparable Br-contents for both coatings. Small differences can be observed for the C-, O-, and Si-content but these are challenging to explain. Additionally, the high-resolution XPS spectra are very similar, although small differences can be observed. The comparison of relevant spectra for both coatings can be found in the Supporting Information (Figure S5). The Br 3d spectra overlapped almost completely, which indicates a similar selective functionality for the ppHMDSO coating that reacted with BrPTCS as for its air-plasma-activated equivalent. The absence of a F-contribution in the atomic composition suggests that the ppHMDSO coating is stable in toluene and ethanol at 70 °C for 3 h, as also observed for the apa-ppHMDSO layers up until 6 h. In line with this observation,

https://doi.org/10.1021/acsami.1c18223
ACS Appl. Mater. Interfaces 2022, 14, 4620−4636

Table 4. XPS Atomic Composition of Different Coatings before and after Incubation for 5 min in Acetone and Subsequently 5 min in Ethanol, Both under Ultrasonification

	C%	O%	Si%	N%
Apa-ppHMDSO APTES 3h Tol	53.3 ± 2.4	23.9 ± 0.9	13.1 ± 1.0	9.7 ± 0.6
incubated	59.6 ± 0.2	21.1 ± 0.3	10.0 ± 0.2	9.3 ± 0.5
Apa-ppHMDSO APTES 3h EtOh	53.1 ± 0.5	22.9 ± 0.4	12.6 ± 0.2	11.3 ± 0.2
incubated	39.7 ± 0.8	38.4 ± 0.5	17.7 ± 0.1	4.3 ± 0.3
	C%	O%	Si%	Br%
ppHMDSO BrPTCS 30 min Tol	49.2 ± 0.4	27.9 ± 0.5	15.9 ± 1.5	7.0 ± 1.3
incubated	49.9 ± 0.8	27.1 ± 0.7	22.6 ± 0.5	0.5 ± 0.2
Apa-ppHMDSO BrPTCS 30 min Tol	53.4 ± 1.2	25.7 ± 0.9	13.0 ± 0.4	7.9 ± 0.6
incubated	44.5 ± 3.0	30.3 ± 2.9	16.6 ± 1.2	8.6 ± 1.0

the coating is also stable in toluene at room temperature up until 6 h. This indicates a significant amount of cross-linking in the coating as the coating would be otherwise dissolved under these relatively harsh conditions. This illustrates that HMDSO requires a significantly lower power to monomer mass ratio to obtain cross-linked films as compared to other monomers used in similar setups. For HMDSO, this ratio was equal to 1.8 W/11 mg/min, while acrylic acid and *N,N*-dimethylacrylamide required more than 20 W for a monomer flow of 4.2 and 3.3 mg/min, respectively.[4,53]

However, this does not prove the stability of the entire functional coating layer, as the obtained coating can still fail due to insufficient cross-linking in between APTES or BrPTCS molecules or weak attachment to the ppHMDSO layer. To evaluate this stability, the resulting coatings are ultrasonificated for 5 min in acetone and in ethanol, which is a conventional method for the removal of weakly bound, physically adsorbed organosilicon layers.[47,54] Table 4 summarizes the stability evaluation by XPS atomic composition calculation for the plasma-activated ppHMDSO coatings reacted with APTES in both solvents and the BrPTCS-reacted ppHMDSO and apa-ppHMDSO layers, as a similar selective functional Br-containing coating was obtained after reaction on both ppHMDSO and apa-ppHMDSO coatings.

From Table 4, it can be observed that the N-content does not change significantly for the APTES-reacted coating that was prepared in toluene at 70 °C, while the C-content increases and O- and Si-contents decrease accordingly. This indicates that the solvent incubation still results in a modification of the layer without influencing the relative N-content. When the APTES reaction is performed in ethanol at 70 °C, a different behavior is observed as the N- and C-content significantly decrease, while the O- and Si-contents significantly increase accordingly. This suggests a thickness decrease of the APTES-derived layer on top of the air-plasma-activated ppHMDSO coating, resulting in an increased contribution of the latter layer in the XPS measurement. However, still an APTES-derived layer should remain as a N-content of 4.3% is still observed. This content is more similar to the previously mentioned studies focusing on APTES modification on glass or silicon.[47−49] The low standard deviations suggest a quite homogeneous coating removal instead of a localized washing. The differential stability in between the APTES-based layer deposited in ethanol and toluene might be explained by the higher expected presence of water in the former solvent. This could result in the formation of polymerized fragments in the solvent which can subsequently be incorporated in the coating without being covalently bonded. Additionally, ethanol could influence the equilibrium of the different reactions that will lead to siloxane-bond formation (Si−O−C hydrolysis, condensation of 2 Si−OH groups, ...), leading to a lower degree of cross-linking in the deposited film as compared with the reactions in toluene.

The BrPTCS-based layers on the two coatings show a very different behavior upon ultrasonification, as the Br-content disappears almost completely for the BrPTCS-functionalized ppHMDSO coating, while the Br-content remains similar after ultrasonification of the BrPTCS-functionalized apa-ppHMDSO coating. The former observation indicates an almost complete removal of the BrPTCS-based layer, which is further demonstrated by the similarity between the resulting atomic composition and the atomic composition of the ppHMDSO coating displayed in Table 2. This suggests that the silanization agent did not react significantly with the coating but rather formed a layer on top of it. This implies that a low amount of reactive groups like silanols are present on the ppHMDSO surface. This can also explain the low reactivity toward APTES, as observed in Table 3. Moreover, it indicates that ultrasonification in acetone and ethanol is capable of dissolving organosilicon layers, which proves the stability of the other three examined layers. The C-content of the ultrasonificated BrPTCS-reacted apa-ppHMDSO coating decreases, while the O- and Si-content decreases accordingly. This indicates that the solvent incubation still results in a modification of the layer without influencing the relative Br-content. This is similar to the APTES-modification in toluene at 70 °C of the coating, although the atomic composition changes in the opposite direction. The absence of any F-content proves that the plasma polymer coating is also stable upon ultrasonification for a short period in ethanol and acetone. Figure 5 displays the comparison of the high-resolution XPS spectra of the three different silanized apa-ppHMDSO coatings and their incubated counterparts.

Figure 5A shows that the high-resolution XPS spectra of the samples that underwent APTES reaction in toluene do not change substantially after ultrasonification, in comparison to their equivalent in ethanol as observed in Figure 5B. In the latter figure, the O 1s and Si 2p spectra show an increased contribution at higher energies. This can be in line with the aforementioned expected thickness decrease of the APTES-based layer, as these alterations can be related to a higher incorporation of the underlying apa-ppHMDSO coating in the XPS measurement. The N 1s spectra suggest that all N atoms are still incorporated as amines after the stability test, although the ultrasonification results in a different ratio of protonated and deprotonated amines. The Br 3d spectra in Figure 5C indicate that all Br atoms are still incorporated as alkyl bromide chains. Further clarifications for the small change in atomic

https://doi.org/10.1021/acsami.1c18223
ACS Appl. Mater. Interfaces 2022, 14, 4620−4636

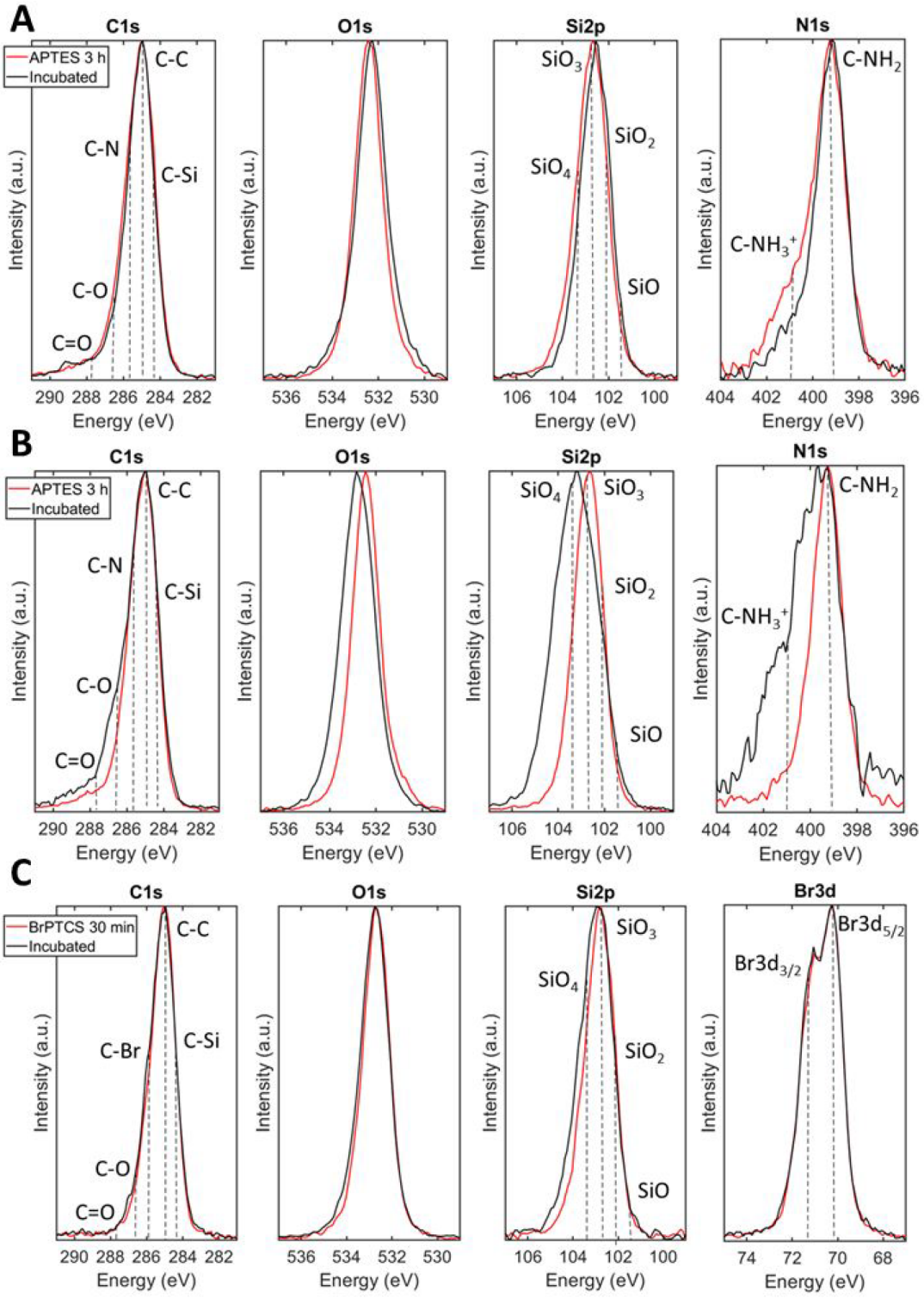

Figure 5. High-resolution XPS spectra for the different silanized apa-ppHMDSO coatings before and after incubation for 5 min in both acetone and ethanol under ultrasonification: (A) APTES in toluene at 70 °C, (B) APTES in ethanol at 70 °C, (C) BrPTCS in toluene at room temperature.

composition and high-resolution XPS spectra would require advanced thickness measurements, which cannot be performed on these coatings. As mentioned before, the coating thickness after 1 min of deposition on glass was equal to 94 ± 19 nm. This variation is typically observed with similar medium-pressure setups, but this complicates the evaluation of small thickness changes after the different reactions.[4,53] Therefore, a further study on the changes in the surface chemistry is outside of the article's scope. As such, it is also not possible to evaluate if the saturation in the surface chemistry, as illustrated in Figures 3 and 4, is caused by the completion of the surface reaction or because of the continuous addition of a layer with similar chemistry.

3.5. Discussion. By combining the observations of the air-plasma-activation influence on the silanization reaction and the stability measurements, some additional conclusions can be

https://doi.org/10.1021/acsami.1c18223
ACS Appl. Mater. Interfaces 2022, 14, 4620−4636

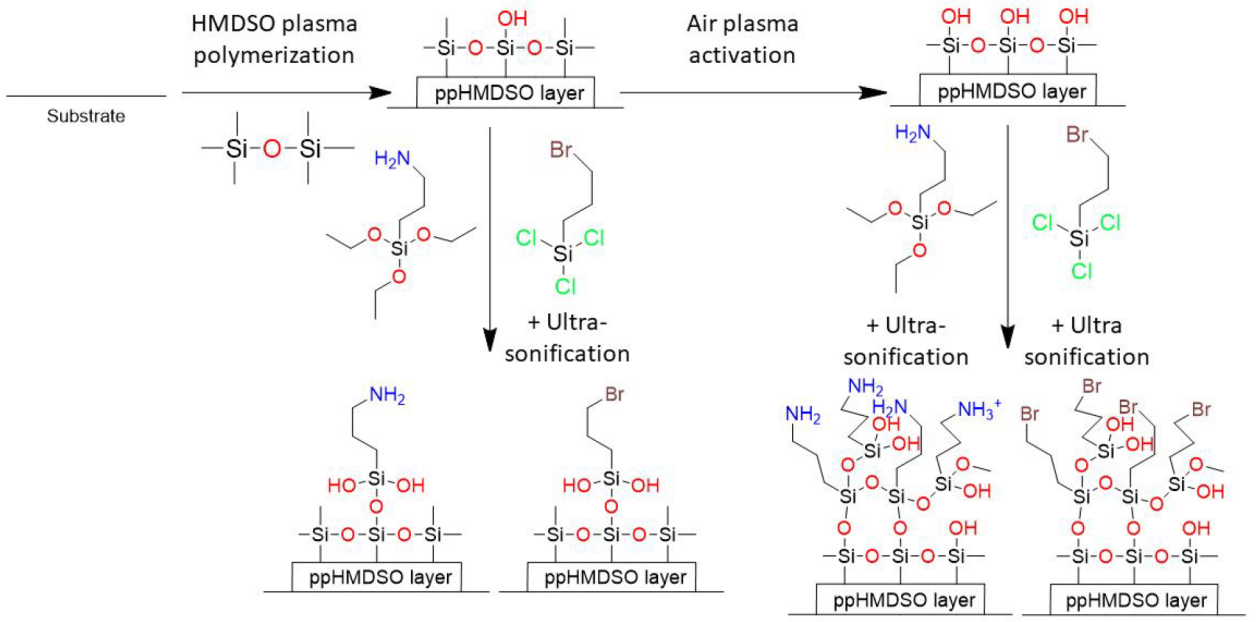

Figure 6. Schematic representation of the observations on the surface chemistry as assessed in this study.

drawn. Figure 6 also schematically summarizes the observations and conclusions made in the previous sections.

It should first be noted that the schematic representation is a simplification without showing the extended siloxane network, the thicker silanization layer that is most likely formed, other surface functionalities like alcohols that may also play a role in the coupling, and the orientation of the functionalities that might not all be the same, as described previously.[54] However, the scheme summarizes the most important observations made in this study. First, it can be seen that the HMDSO plasma polymerization results in a PDMS-like layer with a minimal amount of surface silanol groups, as evidenced by the measurements shown in Tables 3 and 4. Second, the air-plasma-activation step results in more reactive groups on the ppHMDSO surface, of which silanols are the most important. Because of the aforementioned measurements, it can be concluded that this treatment step is necessary to get sufficient connectivity between the ppHMDSO coating and the additional organosilicon layer. The difference in silanization between the apa-ppHMDSO and ppHMDSO coatings also illustrates that the thin plasma-activated layer is stable to a certain extent, as a completely unstable-activated layer would result in silanization of the underlying ppHMDSO coating which resulted in lower N-contents. Third, the APTES- and BrPTCS-based layer on apa-ppHMDSO coatings reacted in toluene at, respectively, 70 °C and room temperature, showed a complete preservation of the functionality as, respectively, the N- or Br-content was similar and the high-resolution XPS spectra evidenced no alterations on the N- and Br-containing functional groups after the stability test. This confirms that both reaction conditions are suitable for the synthesis of stable coatings with selective functionalities. As discussed before, the APTES- and BrPTCS-derived layers were similar on glass and UHMWPE (see Supporting Information (Table S1)), suggesting that stable layers could be deposited on different substrates, which indicates the wide applicability of this functionalization technique. The APTES-based layer on the apa-ppHMDSO coating reacted in ethanol was less stable but still showed selective functionality after the stability evaluation. This illustrates that these coatings could also be used, although a washing step is then needed to remove weakly bound organosilicon particles from the coating. Both selective coatings could be an alternative for classical plasma polymers. The APTES-modified apa-ppHMDSO films can be an alternative for amine-based plasma polymers because of its high primary amine content, which is difficult to achieve for the latter type of coatings. This can be useful for different applications, such as for biosensors.[10] The BrPTCS-based coatings, on the other hand, will mainly differ from bromine-based plasma polymers in its cross-linking degree. Thus, the former coatings will have only primary alkyl bromide groups, while the latter will have secondary and tertiary alkyl bromide groups, as well. This can deteriorate the postmodification capabilities of the latter coating due to steric hindrance, as bromine-based plasma polymers have been used in the past for this purpose.[55,56] An additional feature of plasma polymerization is its capability of depositing relatively smooth subμm films.[23,27,38] Therefore, the influence of the plasma activation and the different reactions on the roughness of the ppHMDSO coating was evaluated by AFM (see section 5 in Supporting Information). The APTES- or BrPTCS-based grafting step resulted in an increase in roughness in comparison to the (air-plasma-activated) plasma polymerized HMDSO coating. However, all coatings had a relatively smooth morphology, as typical Rq values of polymer substrates are often higher.[36,57] This indicates that both selective coatings can indeed be used to replace classical plasma polymers for certain applications.

The main difference between the ppHMDSO-based and the previously reported bromine plasma polymer-based approach is the pending remaining functionality. The former technique results in a coating with the desired functionality and probably some unreacted silanol as the other reactive group, while the latter technique has some remaining alkyl bromides as other reactive functionality. As such, it should always be considered if the presence of alkyl bromides or silanols is unwanted for the intended purpose, but obtaining this selectivity can be seen as a major improvement over standard plasma polymerization processes. It can be expected that the silanol functionalities

https://doi.org/10.1021/acsami.1c18223
ACS Appl. Mater. Interfaces 2022, 14, 4620−4636

will not have an influence for most uses, as this group mainly reacts with Si-based compounds, which are less relevant for biosensor or polymer immobilization applications, for example. Moreover, their presence could be even optimized to an absolute minimum by optimizing the reaction mixture and, as such, obtaining a SAM. Additionally, the coupling reaction in the ppHMDSO-based technique can be performed with a large variation of reaction parameters, as silanization could also be performed at room temperature or in the vapor phase. This could be relevant for the functionalization of thermosensitive substrates, although reaction conditions should be optimized again. Moreover, the surface density of functional groups with the presented technique will mainly depend on the quality of the silanization mixture, whereas the surface density of alkyl bromides will determine the functional group density in the other approach. This makes the latter technique more susceptible to variations in the plasma process, like oxidation of the plasma polymer or extensive monomer fragmentation. For the silanization process, these aspects are less important, as the only prerequisite is the deposition of an organizilicon layer, of which the chemistry can subsequently be altered. This makes the approach presented here more widely applicable, as ppHMDSO coatings have been deposited with a large variety of plasma sources, even at atmospheric pressure.[38,58] Further research should be performed to compare the surface functional group density for both techniques used in this work and conventional plasma polymerization techniques.

At last, it should also be noted that some studies focused on the direct silanization of polymer surfaces, which could result in similar selective functional coatings, although these investigations are mainly focused on aminosilane immobilization. Howarter et al. indicated that a variety of different polymers could be functionalized with APTES, although polystyrene and PTFE could not be silanized.[59] They proposed that the reaction proceeds by initial APTES adsorption (likely through hydrogen bonding by the amine) to the substrate, lateral bond formation, and subsequent multilayer formation, indicating the importance of the primary amine group in the silanization agent. As such, the coating layer is noncovalently immobilized, which can hamper its stability.[59] Castillo et al. illustrated that APTES could also be immobilized on polyesters by transesterification.[60] This occurs however at the expense of polymer degradation and cannot be applied on a variety of substrates. A couple of studies have indicated that plasma activation of the polymer surface prior to silanization could result in covalent grafting of the coating layer on substrates like polystyrene.[54,61] This coupling occurred mainly via hydrolysis-susceptible bonds like imines and silyl ethers, which can hamper the application range for this immobilization strategy. The ppHMDSO-based surface modification technique of this study can therefore be seen as a significant improvement over the aforementioned approaches as it allows first to functionalize a wider variety of substrates, evidenced in this study by the successful functionalization of PTFE. Second, the coupling between the silanization agent and silanol groups has been developed already for multiple silanization agents, allowing the application of a wider variety of functionalities with a similar functionalization degree.[62−64] Third, the plasma polymer film acts as an intermediate layer that is covalently bonded to both the substrate and the silanization agent-based layer, which should significantly enhance the stability of the total coating under aqueous conditions. Additionally, this technique is more straightforward than optimizing the plasma activation for each substrate for applications in which coating stability is not necessary.

4. CONCLUSION

In this work, the development of substrate-independent coatings with selective primary amine and alkyl bromide functionalities was studied. Therefore, silanol-rich plasma polymer coatings were initially deposited by a two-step process in which HMDSO-based PDMS-like films were first applied, followed by plasma activation with air. These apa-ppHMDSO films were subsequently used for reaction with APTES in ethanol and toluene or with BrPTCS in toluene, which were chosen as functional alkoxy- and trichlorosilane model compounds, respectively. The reaction with both silane coupling agents reached a saturation in surface chemistry as observed by XPS, with a faster stabilization for BrPTCS that is likely due to the higher reactivity of the trichlorosilane groups compared with the trialkoxysilane groups. XPS measurements indicated that selective coating chemistry was obtained, and that besides the desired amine or alkyl bromide functional groups also remaining silanol groups are present in the coating. Moreover, it was proven that the air-plasma-activation step is necessary for successful grafting (determined for one reaction time in the saturation region), as APTES did not react in the same way without the activation step and the BrPTCS-derived layer did not covalently attach to the nonactivated plasma polymer. The APTES- and BrPTCS-based films that were deposited on the apa-ppHMDSO coatings retained the selective surface chemistry after ultrasonification, indicating a stable surface functionalization. Additionally, the ppHMDSO coatings and the thin air-plasma-activated layer were stable under the relatively harsh reaction conditions. In summary, this study established a widely applicable method for the fabrication of surfaces with a variety of chemical functionalities, as a plethora of silanization agents with different functional groups are commercially available. Thus, future applications of such functional coatings could be envisioned in biosensor applications, for biomolecule or polymer immobilization and for the synthesis of antibacterial coatings, among others.[63,65,66]

■ ASSOCIATED CONTENT

Supporting Information

The Supporting Information is available free of charge at https://pubs.acs.org/doi/10.1021/acsami.1c18223.

Scheme of the plasma polymerization setup; electrical characterization of plasma for plasma polymerization and activation; XPS high-resolution spectra comparisons for different conditions; XPS atomic composition of silanized coatings on glass, PTFE, and UHMWPE; morphology of the different coatings (PDF)

■ AUTHOR INFORMATION

Corresponding Authors

Richard Hoogenboom − *Supramolecular Chemistry Group, Centre of Macromolecular Chemistry (CMaC), Department of Organic and Macromolecular Chemistry, Faculty of Sciences, Ghent University, 9000 Ghent, Belgium;* orcid.org/0000-0001-7398-2058; Email: richard.hoogenboom@ugent.be

Nathalie De Geyter − *Research Unit Plasma Technology (RUPT), Department of Applied Physics, Faculty of*

Engineering and Architecture, Ghent University, 9000 Ghent, Belgium; Email: Nathalie.degeyter@ugent.be

Authors

Tim Egghe − *Research Unit Plasma Technology (RUPT), Department of Applied Physics, Faculty of Engineering and Architecture, Ghent University, 9000 Ghent, Belgium; Supramolecular Chemistry Group, Centre of Macromolecular Chemistry (CMaC), Department of Organic and Macromolecular Chemistry, Faculty of Sciences, Ghent University, 9000 Ghent, Belgium*

Rouba Ghobeira − *Research Unit Plasma Technology (RUPT), Department of Applied Physics, Faculty of Engineering and Architecture, Ghent University, 9000 Ghent, Belgium;* orcid.org/0000-0001-6064-2070

Parinaz Saadat Esbah Tabaei − *Research Unit Plasma Technology (RUPT), Department of Applied Physics, Faculty of Engineering and Architecture, Ghent University, 9000 Ghent, Belgium;* orcid.org/0000-0001-6419-2951

Rino Morent − *Research Unit Plasma Technology (RUPT), Department of Applied Physics, Faculty of Engineering and Architecture, Ghent University, 9000 Ghent, Belgium*

Complete contact information is available at: https://pubs.acs.org/10.1021/acsami.1c18223

Notes

The authors declare no competing financial interest.

■ ACKNOWLEDGMENTS

T.E. acknowledges the support of the Research Foundation Flanders (FWO) for a Ph.D. grant strategic basic research (3S33118). Rouba Ghobeira would like to thank the FWO (grant number 12ZC720N) for financing her postdoctoral position. Richard Hoogenboom acknowledges Ghent University and FWO for continuous financial support.

■ REFERENCES

(1) Zhang, C.; Ma, M.-Q.; Chen, T.-T.; Zhang, H.; Hu, D.-F.; Wu, B.-H.; Ji, J.; Xu, Z.-K. Dopamine-Triggered One-Step Polymerization and Codeposition of Acrylate Monomers for Functional Coatings. *ACS Appl. Mater. Interfaces* **2017**, *9* (39), 34356−34366.

(2) Wei, Q.; Haag, R. Universal Polymer Coatings and their Representative Biomedical Applications. *Materials Horizons* **2015**, *2* (6), 567−577.

(3) Desmet, T.; Morent, R.; De Geyter, N.; Leys, C.; Schacht, E.; Dubruel, P. Nonthermal Plasma Technology as a Versatile Strategy for Polymeric Biomaterials Surface Modification: A Review. *Biomacromolecules* **2009**, *10* (9), 2351−2378.

(4) Egghe, T.; Cools, P.; Van Guyse, J. F. R.; Asadian, M.; Khalenkow, D.; Nikiforov, A.; Declercq, H.; Skirtach, A. G.; Morent, R.; Hoogenboom, R.; De Geyter, N. Water-Stable Plasma-Polymerized N,N-Dimethylacrylamide Coatings to Control Cellular Adhesion. *ACS Appl. Mater. Interfaces* **2020**, *12* (2), 2116−2128.

(5) Ryu, J. H.; Messersmith, P. B.; Lee, H. Polydopamine Surface Chemistry: A Decade of Discovery. *ACS Appl. Mater. Interfaces* **2018**, *10* (9), 7523−7540.

(6) Deilmann, M.; Theiß, S.; Awakowicz, P. Pulsed Microwave Plasma Polymerization of Silicon Oxide Films: Application of Efficient Permeation Barriers on Polyethylene Terephthalate. *Surf. Coat. Technol.* **2008**, *202* (10), 1911−1917.

(7) Wu, Y. J.; Timmons, R. B.; Jen, J. S.; Molock, F. E. Non-fouling Surfaces Produced by Gas Phase Pulsed Plasma Polymerization of an Ultra Low Molecular Weight Ethylene Oxide Containing Monomer. *Colloids Surf., B* **2000**, *18* (3), 235−248.

(8) Muguruma, H.; Karube, I. Plasma-polymerized Films for Biosensors. *TrAC Trends in Analytical Chemistry* **1999**, *18* (1), 62−68.

(9) Kingshott, P.; Thissen, H.; Griesser, H. J. Effects of Cloud-point Grafting, Chain Length, and Density of PEG layers on Competitive Adsorption of Ocular Proteins. *Biomaterials* **2002**, *23* (9), 2043−2056.

(10) Manakhov, A.; Makhneva, E.; Skládal, P.; Nečas, D.; Čechal, J.; Kalina, L.; Eliáš, M.; Zajíčková, L. The Robust Bio-immobilization Based on Pulsed Plasma Polymerization of Cyclopropylamine and Glutaraldehyde Coupling Chemistry. *Appl. Surf. Sci.* **2016**, *360*, 28−36.

(11) Brétagnol, F.; Lejeune, M.; Papadopoulou-Bouraoui, A.; Hasiwa, M.; Rauscher, H.; Ceccone, G.; Colpo, P.; Rossi, F. Fouling and non-fouling surfaces produced by plasma polymerization of ethylene oxide monomer. *Acta Biomaterialia* **2006**, *2* (2), 165−172.

(12) Bazaka, K.; Jacob, M. V.; Chrzanowski, W.; Ostrikov, K. Anti-bacterial Surfaces: Natural Agents, Mechanisms of Action, and Plasma Surface Modification. *RSC Adv.* **2015**, *5* (60), 48739−48759.

(13) Friedrich, J. F.; Mix, R.; Schulze, R.-D.; Meyer-Plath, A.; Joshi, R.; Wettmarshausen, S. New Plasma Techniques for Polymer Surface Modification with Monotype Functional Groups. *Plasma Processes and Polymers* **2008**, *5* (5), 407−423.

(14) Thiry, D.; Pouyanne, M.; Cossement, D.; Hemberg, A.; Snyders, R. Surface Engineering of Bromine-Based Plasma Polymer Films: A Step toward High Thiol Density Containing Organic Coatings. *Langmuir* **2018**, *34* (26), 7655−7662.

(15) Chen, R. T.; Muir, B. W.; Such, G. K.; Postma, A.; Evans, R. A.; Pereira, S. M.; McLean, K. M.; Caruso, F. Surface "Click" Chemistry on Brominated Plasma Polymer Thin Films. *Langmuir* **2010**, *26* (5), 3388−3393.

(16) Truica-Marasescu, F.; Wertheimer, M. R. Nitrogen-Rich Plasma-Polymer Films for Biomedical Applications. *Plasma Processes and Polymers* **2008**, *5* (1), 44−57.

(17) Taglietti, A.; Arciola, C. R.; D'Agostino, A.; Dacarro, G.; Montanaro, L.; Campoccia, D.; Cucca, L.; Vercellino, M.; Poggi, A.; Pallavicini, P.; Visai, L. Antibiofilm Activity of a Monolayer of Silver Nanoparticles Anchored to an Amino-silanized Glass Surface. *Biomaterials* **2014**, *35* (6), 1779−1788.

(18) Zhu, M.; Lerum, M. Z.; Chen, W. How to Prepare Reproducible, Homogeneous, and Hydrolytically Stable Amino-silane-derived Layers on Silica. *Langmuir: the ACS journal of surfaces and colloids* **2012**, *28* (1), 416−423.

(19) Asenath Smith, E.; Chen, W. How To Prevent the Loss of Surface Functionality Derived from Aminosilanes. *Langmuir* **2008**, *24* (21), 12405−12409.

(20) McGovern, M. E.; Kallury, K. M. R.; Thompson, M. Role of Solvent on the Silanization of Glass with Octadecyltrichlorosilane. *Langmuir* **1994**, *10* (10), 3607−3614.

(21) Li, Z. F.; Ruckenstein, E. Conductive Surface via Graft Polymerization of Aniline on a Modified Glass Surface. *Synth. Met.* **2002**, *129* (1), 73−83.

(22) Schäfer, J.; Horn, S.; Foest, R.; Brandenburg, R.; Vašina, P.; Weltmann, K.-D. Complex Analysis of SiOxCyHz films Deposited by an Atmospheric Pressure Dielectric Barrier Discharge. *Surf. Coat. Technol.* **2011**, *205*, S330−S334.

(23) Morent, R.; De Geyter, N.; Van Vlierberghe, S.; Dubruel, P.; Leys, C.; Schacht, E. Organic−inorganic Behaviour of HMDSO Films Plasma-polymerized at Atmospheric Pressure. *Surf. Coat. Technol.* **2009**, *203* (10), 1366−1372.

(24) Narimisa, M.; Ghobeira, R.; Onyshchenko, Y.; De Geyter, N.; Egghe, T.; Morent, R. Different Techniques Used for Plasma Modification of Polyolefin Surfaces. In *Plasma Modification of Polyolefins: Synthesis, Characterization and Applications*; Baneesh, N. S., Sari, P. S., Vackova, T., Thomas, S., Eds.; Springer International Publishing: Cham, 2022; pp 15−56.

(25) Prikryl, R.; Otrisal, P.; Obsel, V.; Svorc, L.; Karkalic, R.; Buk, J. Protective Properties of a Microstructure Composed of Barrier Nanostructured Organics and SiO(x) Layers Deposited on a Polymer Matrix. *Nanomaterials (Basel)* **2018**, *8* (9), 679.

(26) Ma, C.; Wang, L.; Nikiforov, A.; Onyshchenko, Y.; Cools, P.; Ostrikov, K.; De Geyter, N.; Morent, R. Atmospheric-pressure Plasma Assisted Engineering of Polymer Surfaces: From High Hydrophobicity to Superhydrophilicity. *Appl. Surf. Sci.* **2021**, *535*, 147032.
(27) Cools, P.; Van Vrekhem, S.; De Geyter, N.; Morent, R. The Use of DBD Plasma Treatment and Polymerization for the Enhancement of Biomedical UHMWPE. *Thin Solid Films* **2014**, *572*, 251−259.
(28) Cools, P.; Sainz-García, E.; Geyter, N. D.; Nikiforov, A.; Blajan, M.; Shimizu, K.; Alba-Elías, F.; Leys, C.; Morent, R. Influence of DBD Inlet Geometry on the Homogeneity of Plasma-Polymerized Acrylic Acid Films: The Use of a Microplasma−Electrode Inlet Configuration. *Plasma Processes and Polymers* **2015**, *12* (10), 1153−1163.
(29) Van Guyse, J. F. R.; Cools, P.; Egghe, T.; Asadian, M.; Vergaelen, M.; Rigole, P.; Yan, W.; Benetti, E. M.; Jerca, V.-V.; Declercq, H.; Coenye, T.; Morent, R.; Hoogenboom, R.; De Geyter, N. Influence of the Aliphatic Side Chain on the Near Atmospheric Pressure Plasma Polymerization of 2-Alkyl-2-oxazolines for Biomedical Applications. *ACS Appl. Mater. Interfaces* **2019**, *11* (34), 31356−31366.
(30) Cools, P.; Asadian, M.; Nicolaus, W.; Declercq, H.; Morent, R.; De Geyter, N. Surface Treatment of PEOT/PBT (55/45) with a Dielectric Barrier Discharge in Air, Helium, Argon and Nitrogen at Medium Pressure. *Materials (Basel)* **2018**, *11* (3), 391.
(31) Alexander, M. R.; Short, R. D.; Jones, F. R.; Michaeli, W.; Blomfield, C. J. A Study of HMDSO/O2 Plasma Deposits Using a High-sensitivity and -energy Resolution XPS Instrument: Curve Fitting of the Si 2p Core Level. *Appl. Surf. Sci.* **1999**, *137* (1), 179−183.
(32) López, G. P.; Castner, D. G.; Ratner, B. D. XPS O 1s Binding Energies for Polymers Containing Hydroxyl, Ether, Ketone and Ester groups. *Surf. Interface Anal.* **1991**, *17* (5), 267−272.
(33) Jagst, E. Surface Functional Group Characterization Using Chemical Derivatization X-ray Photoelectron Spectroscopy (CD-XPS). Ph.D. Thesis, Freie Universität Berlin, Berlin, 2011.
(34) Vasilev, K.; Michelmore, A.; Griesser, H. J.; Short, R. D. Substrate Influence on the Initial Growth Phase of Plasma-deposited Polymer Films. *Chem. Commun.* **2009**, No. 24, 3600−3602.
(35) Esbah Tabaei, P. S.; Ghobeira, R.; Cools, P.; Rezaei, F.; Nikiforov, A.; Morent, R.; De Geyter, N. Comparative Study Between In-plasma and Post-plasma Chemical Processes Occurring at the Surface of UHMWPE Subjected to Medium Pressure Ar and N2 Plasma Activation. *Polymer* **2020**, *193*, 122383.
(36) Van Vrekhem, S.; Vloebergh, K.; Asadian, M.; Vercruysse, C.; Declercq, H.; Van Tongel, A.; De Wilde, L.; De Geyter, N.; Morent, R. Improving the Surface Properties of an UHMWPE Shoulder Implant with an Atmospheric Pressure Plasma Jet. *Sci. Rep.* **2018**, *8* (1), 4720.
(37) Alexander, M. R.; Short, R. D.; Jones, F. R.; Stollenwerk, M.; Zabold, J.; Michaeli, W. An X-ray Photoelectron Spectroscopic Investigation into the Chemical Structure of Deposits Formed from Hexamethyldisiloxane/Oxygen Plasmas. *J. Mater. Sci.* **1996**, *31* (7), 1879−1885.
(38) Morent, R.; De Geyter, N.; Van Vlierberghe, S.; Dubruel, P.; Leys, C.; Gengembre, L.; Schacht, E.; Payen, E. Deposition of HMDSO-based Coatings on PET Substrates Using an Atmospheric Pressure Dielectric Barrier Discharge. *Prog. Org. Coat.* **2009**, *64* (2), 304−310.
(39) Ghobeira, R.; Philips, C.; Declercq, H.; Cools, P.; De Geyter, N.; Cornelissen, R.; Morent, R. Effects of Different Sterilization Methods on the Physico-chemical and Bioresponsive Properties of Plasma-treated Polycaprolactone Films. *Biomedical Materials* **2017**, *12* (1), 015017.
(40) Hong, S. M.; Kim, S. H.; Kim, J. H.; Hwang, H. I. Hydrophilic Surface Modification of PDMS Using Atmospheric RF Plasma. *Journal of Physics: Conference Series* **2006**, *34*, 656−661.
(41) Chaiwong, C.; Rachtanapun, P.; Sarapirom, S.; Boonyawan, D. Plasma Polymerization of Hexamethyldisiloxane: Investigation of the Effect of Carrier Gas related to the Film Properties. *Surf. Coat. Technol.* **2013**, *229*, 12−17.
(42) Matinlinna, J. P.; Vallittu, P. K. Bonding of Resin Composites to Etchable Ceramic Surfaces − an Insight Review of the Chemical Aspects on Surface Conditioning. *Journal of Oral Rehabilitation* **2007**, *34* (8), 622−630.
(43) Der Voort, P. V.; Vansant, E. F. Silylation of the Silica Surface A Review. *Journal of Liquid Chromatography & Related Technologies* **1996**, *19* (17−18), 2723−2752.
(44) Weetall, H. H. Preparation of Immobilized Proteins Covalently Coupled through Silane Coupling Agents to Inorganic Supports. *Appl. Biochem. Biotechnol.* **1993**, *41* (3), 157−188.
(45) Qin, M.; Hou, S.; Wang, L.; Feng, X.; Wang, R.; Yang, Y.; Wang, C.; Yu, L.; Shao, B.; Qiao, M. Two Methods for Glass Surface Modification and their Application in Protein Immobilization. *Colloids Surf., B* **2007**, *60* (2), 243−249.
(46) Yue, X.; Feng, S.; Li, S.; Jing, Y.; Shao, C. Bromopropyl Functionalized Silica Nanofibers for Effective Removal of Trace Level Dieldrin from Water. *Colloids Surf., A* **2012**, *406*, 44−51.
(47) Seitz, O.; Chehimi, M. M.; Cabet-Deliry, E.; Truong, S.; Felidj, N.; Perruchot, C.; Greaves, S. J.; Watts, J. F. Preparation and Characterisation of Gold Nanoparticle Assemblies on Silanised Glass Plates. *Colloids Surf., A* **2003**, *218* (1), 225−239.
(48) Min, H.; Girard-Lauriault, P.-L.; Gross, T.; Lippitz, A.; Dietrich, P.; Unger, W. E. S. Ambient-ageing Processes in Amine Self-assembled Monolayers on Microarray Slides as Studied by ToF-SIMS with Principal Component Analysis, XPS, and NEXAFS Spectroscopy. *Anal. Bioanal. Chem.* **2012**, *403* (2), 613−623.
(49) Brizzolara, R. A.; Stamper, D. M. The Effect of Covalent Surface Immobilization on the Bactericidal Efficacy of a Quaternary Ammonium Compound. *Surf. Interface Anal.* **2007**, *39* (7), 559−566.
(50) Zheng, S.; Yang, Q.; Mi, B. Novel Antifouling Surface with Improved Hemocompatibility by Immobilization of Polyzwitterions onto Silicon via Click Chemistry. *Appl. Surf. Sci.* **2016**, *363*, 619−626.
(51) Siow, K. S.; Britcher, L.; Kumar, S.; Griesser, H. J. Plasma Methods for the Generation of Chemically Reactive Surfaces for Biomolecule Immobilization and Cell Colonization - A Review. *Plasma Processes and Polymers* **2006**, *3* (6−7), 392−418.
(52) Papirer, E.; Lacroix, R.; Donnet, J.-B.; Nanse, G.; Fioux, P. XPS Study of the Halogenation of Carbon Black-part 1. Bromination. *Carbon* **1994**, *32* (7), 1341−1358.
(53) Cools, P.; Declercq, H.; De Geyter, N.; Morent, R. A Stability Study of Plasma Polymerized Acrylic Acid Films. *Appl. Surf. Sci.* **2018**, *432*, 214−223.
(54) Sunkara, V.; Cho, Y.-K. Aminosilane Layers on the Plasma Activated Thermoplastics: Influence of Solvent on its Structure and Morphology. *J. Colloid Interface Sci.* **2013**, *411*, 122−128.
(55) McGettrick, J. D.; Crockford, T.; Schofield, W. C. E.; Badyal, J. P. S. Bromine-containing Functional Nanolayers for Biomolecule Immobilization. *Appl. Surf. Sci.* **2009**, *256* (3), S30−S34.
(56) Hirsch, U.; Ruehl, M.; Teuscher, N.; Heilmann, A. Antifouling Coatings via Plasma Polymerization and Atom Transfer Radical Polymerization on Thin Film Composite Membranes for Reverse Osmosis. *Appl. Surf. Sci.* **2018**, *436*, 207−216.
(57) Van Deynse, A.; De Geyter, N.; Leys, C.; Morent, R. Influence of Water Vapor Addition on the Surface Modification of Polyethylene in an Argon Dielectric Barrier Discharge. *Plasma Processes and Polymers* **2014**, *11* (2), 117−125.
(58) Lommatzsch, U.; Ihde, J. Plasma Polymerization of HMDSO with an Atmospheric Pressure Plasma Jet for Corrosion Protection of Aluminum and Low-Adhesion Surfaces. *Plasma Processes and Polymers* **2009**, *6* (10), 642−648.
(59) Howarter, J. A.; Youngblood, J. P. Surface Modification of Polymers with 3-Aminopropyltriethoxysilane as a General Pretreatment for Controlled Wettability. *Macromolecules* **2007**, *40* (4), 1128−1132.
(60) Castillo, G. A.; Wilson, L.; Efimenko, K.; Dickey, M. D.; Gorman, C. B.; Genzer, J. Amidation of Polyesters Is Slow in Nonaqueous Solvents: Efficient Amidation of Poly(ethylene tereph-

https://doi.org/10.1021/acsami.1c18223
ACS Appl. Mater. Interfaces 2022, 14, 4620−4636

thalate) with 3-Aminopropyltriethoxysilane in Water for Generating Multifunctional Surfaces. *ACS Appl. Mater. Interfaces* **2016**, *8* (51), 35641−35649.
(61) North, S. H.; Lock, E. H.; Cooper, C. J.; Franek, J. B.; Taitt, C. R.; Walton, S. G. Plasma-Based Surface Modification of Polystyrene Microtiter Plates for Covalent Immobilization of Biomolecules. *ACS Appl. Mater. Interfaces* **2010**, *2* (10), 2884−2891.
(62) Thiry, D.; Francq, R.; Cossement, D.; Guerin, D.; Vuillaume, D.; Snyders, R. Establishment of a Derivatization Method To Quantify Thiol Function in Sulfur-Containing Plasma Polymer Films. *Langmuir* **2013**, *29* (43), 13183−13189.
(63) Zhang, Z.; Chao, T.; Chen, S.; Jiang, S. Superlow Fouling Sulfobetaine and Carboxybetaine Polymers on Glass Slides. *Langmuir* **2006**, *22* (24), 10072−10077.
(64) Dong, Y.; Zhu, X.; Shi, F.; Nie, J. Surface Photo-anchored PNIPAM Crosslinked Membrane on Glass Substrate by Covalent Bonds. *Appl. Surf. Sci.* **2014**, *307*, 7−12.
(65) Godoy-Gallardo, M.; Mas-Moruno, C.; Yu, K.; Manero, J. M.; Gil, F. J.; Kizhakkedathu, J. N.; Rodriguez, D. Antibacterial Properties of hLf1−11 Peptide onto Titanium Surfaces: A Comparison Study Between Silanization and Surface Initiated Polymerization. *Biomacromolecules* **2015**, *16* (2), 483−496.
(66) Jang, L.-S.; Liu, H.-J. Fabrication of Protein Chips Based on 3-aminopropyltriethoxysilane as a Monolayer. *Biomed. Microdevices* **2009**, *11* (2), 331−338.

https://doi.org/10.1021/acsami.1c18223
ACS Appl. Mater. Interfaces 2022, 14, 4620−4636